Influence of compaction direction on performance characteristics of roller-compacted HMA specimens

Bernhard Hofko[a], Ronald Blab[a] & Alexander Alisov[b]

[a] Research Center of Road Engineering, Institute of Transportation, Vienna University of Technology, Gusshausstrasse 28/E230/3, 1040, Vienna, Austria

[b] Braunschweig Pavement Engineering Centre, University of Technology Braunschweig, Beethovenstraße 51b, 38106, Braunschweig, Germany
Published online: 09 Jun 2014.

PLEASE SCROLL DOWN FOR ARTICLE

Taylor & Francis
Taylor & Francis Group

Influence of compaction direction on performance characteristics of roller-compacted HMA specimens

Bernhard Hofko[a*], Ronald Blab[a1] and Alexander Alisov[b2]

[a]Research Center of Road Engineering, Institute of Transportation, Vienna University of Technology, Gusshausstrasse 28/E230/3, 1040 Vienna, Austria; [b]Braunschweig Pavement Engineering Centre, University of Technology Braunschweig, Beethovenstraße 51b, 38106 Braunschweig, Germany

Hot mix asphalt (HMA) slabs produced by roller compaction can be used to core and cut specimens for further testing. The relation between the direction of compaction and testing in the laboratory is not always the same relation as it is between the direction of compaction and actual loading in the field. This paper presents outcomes of a study analysing the influence of the compaction direction on performance characteristics of roller-compacted HMA specimens. Performance parameters of a base layer mix are obtained from performance-based test methods, including high-temperature, stiffness, fatigue and low-temperature tests. The relation between direction of compaction and specimen testing is varied in all three dimensions to find relevant influences. From the results, it can be concluded that all obtained performance parameters are sensitive to the anisotropy of the material due to compaction, especially for stiffness and fatigue performance. For the high-temperature performance, specimens from path- and force-controlled compaction were compared. The applied compaction work rather than the compaction method is linked to the difference in the corresponding results. The uniformity of the compaction in terms of the variation of bulk density of the specimens reflects on the scattering of test results.

Keywords: performance-based test methods; compaction; hot mix asphalt

1. Introduction

Achieving consistency in compaction, both in the laboratory and in the field, is necessary to obtain reliable correlation between hot mix asphalt (HMA) laboratory performance and the observed in-service behaviour. Different laboratory compaction methods may produce volumetrically identical specimens but with widely varying mechanical performance (Brown and Gibb 1999, Renken 2000, Iwama *et al.* 2007). Reason is that the method of compaction has an influence on the aggregate orientation and therefore on the performance itself (Masad *et al.* 1999, Hunter *et al.* 2004). Airey *et al.* (2005) found that the roller compaction used to produce HMA slabs in the laboratory provides the best correlation with field specimens in terms of internal aggregate structure and mechanical properties.

Still, for one specific compaction method, performance indicators show anisotropy. Masad *et al.* (2002) states that stiffness of asphalt specimens differ up to 30% depending on the direction of testing.

In this paper, the effect of the direction of compaction and the orientation of the specimens cored and cut from the compacted HMA slab on performance parameters of the mix are investigated. Also, the compaction method was varied to compare force- and path-controlled compaction. For the preparation of the HMA slabs, the roller compaction according to EN 12697-33 (2007) was used.

To fully describe the characteristics of the mix, the research programme included tests to assess

- high-temperature [triaxial cyclic compression test (TCCT) according to EN 12697-25],
- stiffness and fatigue [cyclic indirect tension test (IT-CY) according to FGSV AL Sp-Asphalt 09 (2009) and EN 12697-24] and
- low-temperature [temperature stress restrained specimen test (TSRST) and uniaxial tension stress test (UTST) according to prEN 12697-46 (2009)] performance.

2. Materials

The mix type used in this study was chosen to represent a base layer asphalt concrete (AC base) commonly used in Austria with a maximum aggregate size of 22 mm. It is known that effects of anisotropy tend to increase with increasing aggregate size in the mix. The base layer is specified as an AC 22 base 50/70 according to EN 13108-1 (2006). Details are listed in Table 1. Figure 1 shows the grading curve.

3. Specimen preparation and test programme

For the preparation of the specimens, the mix was produced in a reverse-rotation compulsory mixer according to EN 12697-35 (2007). The HMA slabs were

*Corresponding author. Email: bernhard.hofko@tuwien.ac.at

Table 1. Mix design.

Type	AC 22 base 50/70
Binder	Pen50/70, unmodified
Binder content (optimised according to Marshall)	4.5% (m/m)
Content of air voids	3.5% (v/v)
Maximum density	2616 (kg/m^3)
Bulk density	2524 (kg/m^3)
Aggregate type	Limestone

compacted by two different roller compactors according to EN 12697-33 (2007) to produce slabs with dimensions 500 mm × 260 mm for high-temperature and stiffness/fatigue tests and 320 mm × 260 mm for low-temperature tests. In general, the compaction was path-controlled. The necessary mass of mix was derived from the aimed volume of the slab and the target density. The compaction was then carried out by a path-controlled precompaction phase and a path-controlled main phase to the target height of the slab. In the path-controlled compaction, the roller compacts the HMA slab to a target height with a constant change in height per cycle (0.3 mm/cycle).

A smaller part of the slabs was produced by force-controlled compaction to compare these two methods. In the force-controlled compaction, the roller compacts the HMA slabs with a constant increase in force per cycle for a specified number of cycles, followed by a constant decrease in force per cycle with the same rate. For force-controlled compaction, it is necessary to carry out pre-tests to derive the change in force per cycle and the number of cycles to make sure that the HMA slab is compacted to the target density. In this study, the change in force per cycle was determined as 1.3 kN/cycle for a number of 15 cycles. Table 2 shows the dimensions of the slabs produced for the study.

To analyse differences in the performance characteristics as a function of compaction direction, different patterns (i.e. orientation of specimen testing vs. orientation of compaction) were used when the specimens were cut and cored. Figure 2 shows the coordinate system set for compaction. The *x*-axis is orthogonal to the roller path and the compaction force. The *y*-axis runs along the roller path, and the *z*-axis represents the direction of the compaction force. Also depicted in Figure 2 is a scheme of specimens used for different test types. In addition, the direction of the loading is plot, and the direction of the relevant reaction measured in the test.

Table 3 gives an overview of the test programme. For each test type, it is shown which orientations were tested together with the name of the pattern used as an acronym for identification. For example, the $F-Z-Y$ indicates an IT-CY (fatigue test) with the orientation of test loading in *z*-direction and the orientation of the relevant reaction in *y*-direction. The orientation is taken from the coordinate system of compaction (Figure 2). Thus, a link between the compaction and the orientation of testing is achieved. In Table 3, the loading-compaction configuration that matches the situation in a pavement under traffic is highlighted in bold letters for each test type. In theory, for the UTST/TSRST as well as for the TCCT, three variations of the orientation are possible. For the IT-CY, six variations could be tested. For the test programme, those orientations were chosen that represent the situation in the road and the orientations that are commonly used in a laboratory to ensure an efficient and economic production of specimens.

4. Test procedures and results

To quantify the influence of the direction of compaction, the performance of the AC 22 mix was characterised by performance-based tests at low (TSRST and UTST),
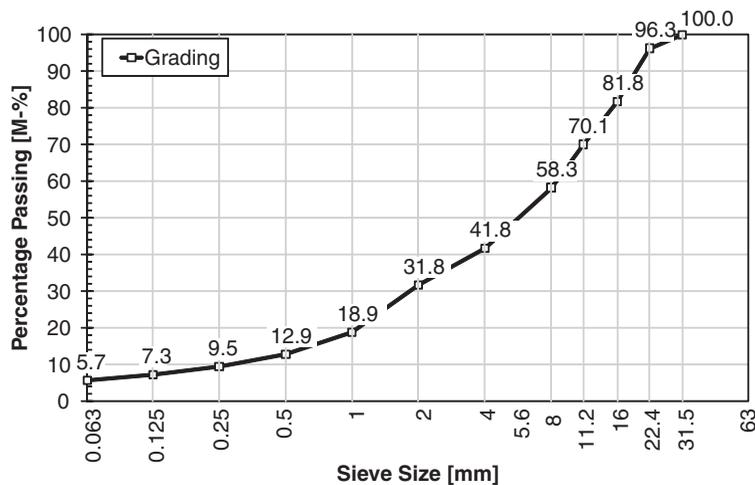
Figure 1. Grading curve.

Table 2. Slab dimensions.

Dimensions (l × w × h)	Compaction	Test type
320 × 260 × 60	Path-controlled	TSRST, UTST
500 × 260 × 150	Path-controlled	IT-CY
500 × 260 × 140	Path-controlled	TCCT
500 × 260 × 220	Path-controlled	TCCT
500 × 260 × 220	Force-controlled	TCCT

intermediate (IT-CY) and high (TCCT) temperatures. The test procedures and results are presented in the following sections.

4.1 *Low-temperature performance*

To assess the resistance to low-temperature cracking, two test types, the TSRST and UTST, were carried out in accordance with prEN 12697-46 (2009).

In the TSRST, a prismatic specimen (60 mm × 60 mm × 225 mm) is glued to two load plates. The length of the specimen is held constant while cooling it down within a climate chamber at a constant rate of 10 K/h starting from 10°C. Due to the restrained shrinkage, the material develops cryogenic stresses due to decreasing temperature. When these cryogenic stresses exceed the tensile strength of the material, the specimen fails by cracking. The temperature of cracking (T_{crack}) and the corresponding cryogenic stress ($\sigma_{cryo,crack}$) are main results of the test. Three specimens are tested to gain T_{crack} and $\sigma_{cryo,crack}$. The test simulates the situation in the road in the cold season after sunset when temperatures especially in alpine regions tend to drop at a high rate. Due to the confinement of a road in longitudinal and transverse direction, cryogenic stresses occur. As the ability for relaxation of viscoelastic flexible pavements (i.e. the relaxation of the

mastic) decreases with a decrease in temperature, at a certain temperature the cryogenic stress reaches the tensile strength of the mix, which leads to (mostly transverse) cracking.

In the UTST, a prismatic specimen (60 mm × 60 mm × 225 mm) is glued to two load plates. The specimen is then cooled down to a target test temperature in a state free of stress and then pulled with a deformation rate of 1 mm/min. The main result is the tensile strength (β_t) at the test temperature. Three specimens are tested to obtain β_t.

By combining the results of the UTST and TSRST at a certain temperature, the tensile strength reserve ($\Delta\beta_t$) can be obtained. It is the difference between the temperature-induced cryogenic stress from the TSRST and the tensile strength from the UTST at the same temperature. The difference between the two stresses is the theoretical strength reserve that a pavement can take in traffic load at a certain temperature before cracking.

4.1.1 *Results*

Both tests were carried out at specimens with an *L–X–X* and an *L–Y–Y* orientation. Table 4 and Figure 3 show relevant results. The *L–X–X* configuration results in a lower cracking temperature at lower cryogenic stresses in the TSRST. Also, the cryogenic stresses at −20°C are lower than for the *L–Y–Y* configuration. The tensile strength at −20°C obtained from the UTST is again smaller for the *L–X–X* specimens. For both test types, the variation of the results in terms of standard deviation (SD) is higher for the *L–X–X* configuration. The tensile strength reserve at −20°C as the main result for the low-temperature behaviour is 2.5 N/mm² (mean value (MV)) for the *L–X–X* with a range from 1.7 to 3.4 N/mm² taking into account the SD. For the *L–Y–Y* configuration, the MV
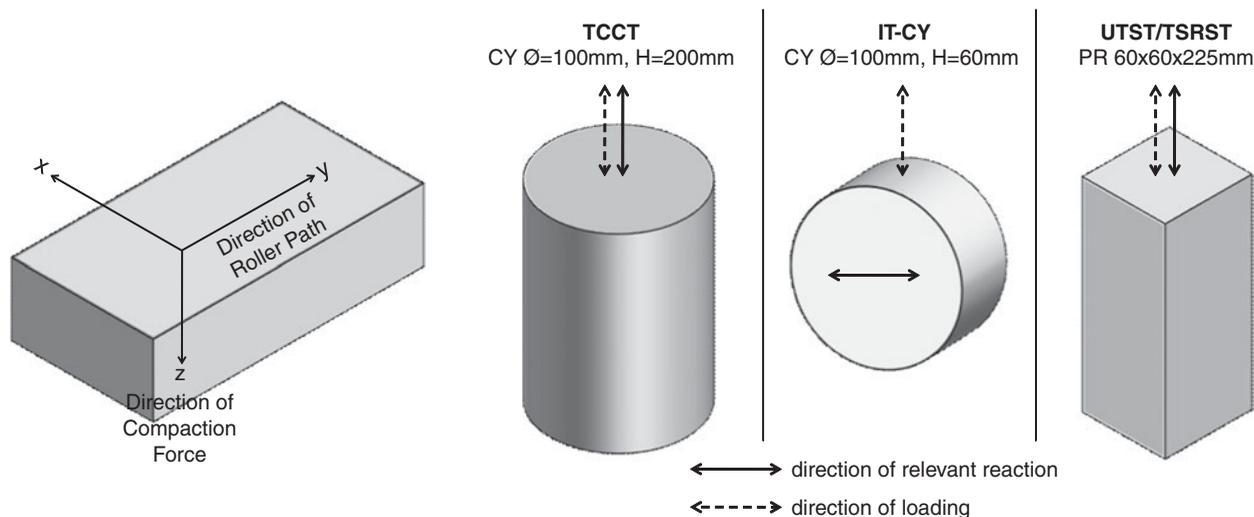
Figure 2. Coordinate system of compaction (left) and principal directions of testing (right).

Table 3. Orientation of specimen and testing.

Test	Direction of coordinate system of compaction		Pattern
	Orientation of loading	Orientation of relevant reaction	
UTST/TSRST	**X**	**X**	**L–X–X**
UTST/TSRST	**Y**	**Y**	**L–Y–Y**
IT-CY	*X*	*Y*	*F–X–Y*
IT-CY	**Z**	**Y**	F–Z–Y
TCCT	**Z**	**Z**	**H–Z–Z**
TCCT	*X*	*X*	*H–X–X*
TCCT	*Y*	*Y*	*H–Y–Y*
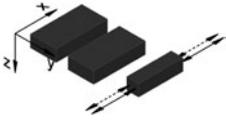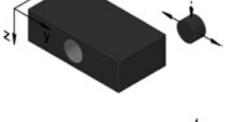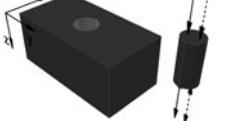
of the reserve is 2.1 N/mm^2 ranging from 1.6 to 2.7 N/mm^2.

This shows that the low-temperature performance is sensitive to the anisotropy of the mix. In transverse orientation ($L–X–X$), the performance is better in terms of temperature-induced stresses (TSRST) as well as of strength reserve, although the tensile strength at low temperatures is smaller than in longitudinal direction ($L–Y–Y$).

Table 4. Low-temperature results.

	$L–X–X$		$L–Y–Y$		$\Delta_{X–X/Y–Y}$ (%)	
	MV	SD	MV	SD	MV	SD
T_{crack} (°C) (TSRST)	-28.5	2.9	-26.7	0.8	-6.3	-72.4
$\sigma_{cryo,crack}$ (N/mm^2) (TSRST)	3.5	0.3	4.0	0.3	14.3	0.0
σ_{cryo} at -20°C (N/mm^2) (TSRST)	1.1	0.6	1.9	0.2	72.7	-66.7
β_t at -20°C (N/mm^2) (UTST)	3.7	0.3	4.0	0.4	8.1	33.3
$\Delta\beta_t$ at -20°C (N/mm^2)	2.5	0.9	2.1	0.6	-16.0	-33.3
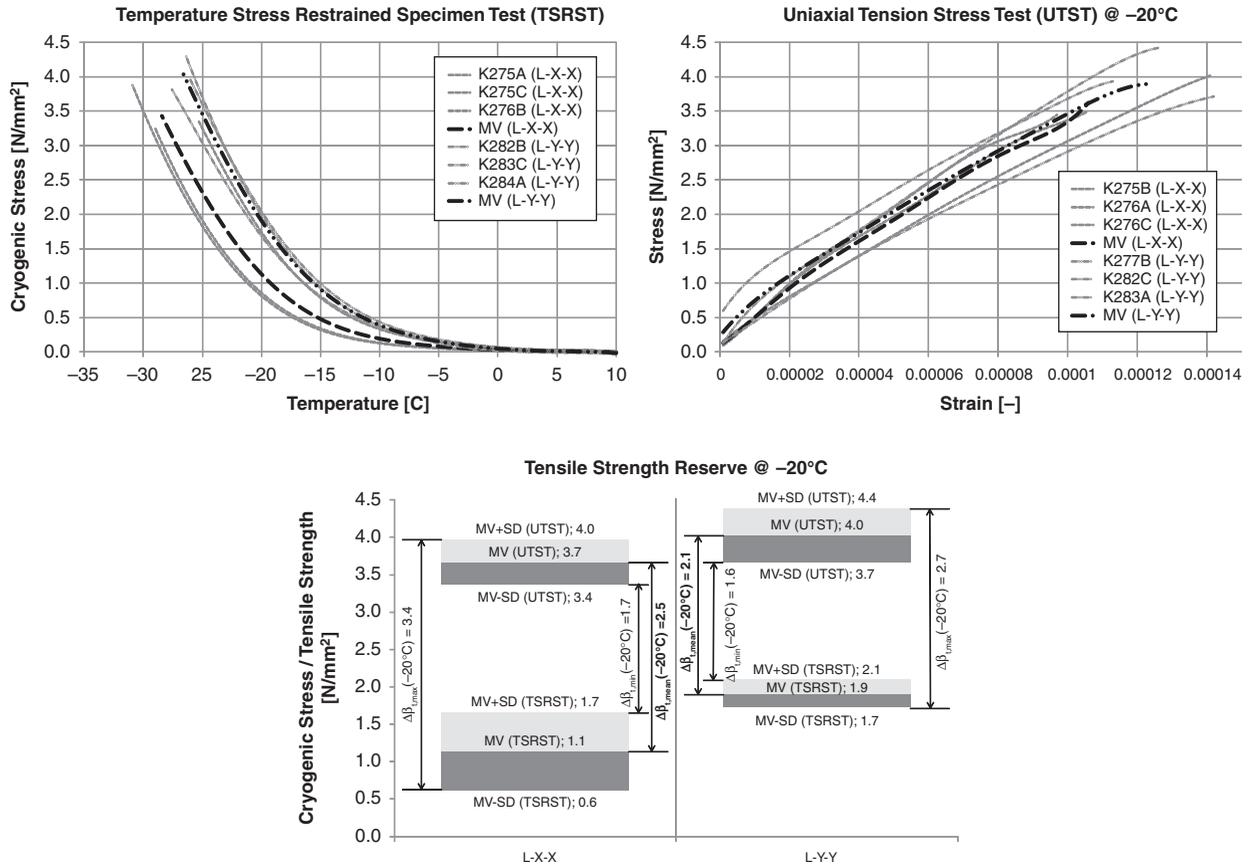
Figure 3.   TSRST results (upper left), UTST results (upper right) and tensile strength reserve (below).

4.2   Stiffness and fatigue performance

For the characterisation of the stiffness and especially the fatigue performance, the IT-CY was carried out. The test procedure is standardised by the German Road and Transportation Research Association (FGSV) in the AL Sp-Asphalt 09 on the basis of EN 12697-24 (2007). A cylindrical specimen is located between two load plates in such a way that a sinusoidal compressive stress is applied to the lateral surface of the specimen. This cyclic compression mainly leads to tensile stresses along the vertical axis which is responsible for fatigue deterioration and finally the failure of the specimen. Within one test procedure, nine specimens are tested (three specimens at three different load levels) at 20°C and a test frequency of 10 Hz. The test is force-controlled with a constant minimum stress of 35 kPa and three different maximum stresses to realise three load levels (in this case 100, 200 and 400 kPa). During the test, the horizontal deformation is recorded by linear variable differential transformers. Due to increasing fatigue, the specimen's stiffness decreases causing increasing horizontal strain as the stress level is held constant. After the test is finished, the dynamic modulus $|E^*|$ is analysed versus the number of load cycles. The point of fatigue is achieved when the

dynamic modulus has reached half the initial dynamic modulus which is obtained after the 100th load cycle. To characterise the fatigue performance, a fatigue function (power function) combining the elastic strain amplitude after the 100th load cycle ($\varepsilon_{el,100}$) versus the number of load cycles until fatigue (N_{fat}) is derived (Figure 4, left).

To characterise and compare the stiffness of specimens, the dynamic modulus after the 100th load cycle is used as a benchmark (Figure 4, right).

4.2.1   Results

In this study, the fatigue performance was derived for the $F-X-Y$ and the $F-Z-Y$ orientation. The $F-Z-Y$ configuration reflects the load situation in a road pavement. The direction of the traffic load is the same as the direction of the compaction force (Z). The traffic load leads to flexural stresses in the pavement with the largest stresses on the bottom of the bound layers in longitudinal direction (Y). Results can be taken from Figure 4 and Table 5. The left diagram in Figure 4 shows the fatigue function for the two tested orientations in log–log scale. The $F-Z-Y$ configurations results in a better fatigue performance with a higher number of load cycles until
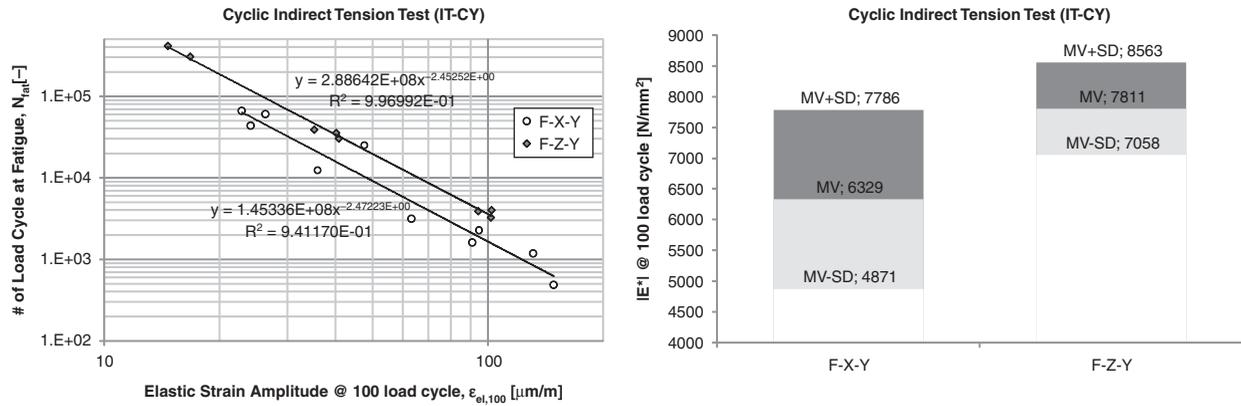
Figure 4.   IT-CY results: fatigue function (left) and stiffness (right).

fatigue. Also, the scattering of test results is significantly lower than for the $F-X-Y$ direction. Table 5 shows that the fatigue performance in $F-Z-Y$ orientation is about 37% higher than in the other direction. Interestingly, the two fatigue functions are parallel in the log–log scale (similar exponents).

The right diagram in Figure 4 provides information about the dynamic stiffness of the mix. Again the $F-Z-Y$ leads to higher results and a smaller variation. In respect to the mean values of $|E^*|$, $F-Z-Y$ is about 23% higher than $F-X-Y$.

It can be concluded that the fatigue and stiffness performance is very sensitive to the anisotropy of the mix

with higher fatigue resistance for the $F-Z-Y$ orientation which reflects the loading situation in the road.

4.3   *High-temperature performance*

The high-temperature performance as the resistance against permanent deformation can be obtained by the TCCT according to EN 12697-25 (2006). A cylindrical specimen is located between two load plates and subjected to a sinusoidal compressive load in axial direction simulating the traffic load. A confining pressure in radial direction represents the confinement of each point in a road by the surrounding pavement structure. The test was

Table 5.   Fatigue and stiffness results.

	$F-X-Y$		$F-Z-Y$		$\Delta_{X-Y/Z-Y}$ (%)	
$\varepsilon_{\text{el,100}}$ at N_{fat} of 1.000 (µm/m)	123		168		36.6	
$\varepsilon_{\text{el,100}}$ at N_{fat} of 10.000 (µm/m)	48		66		37.5	
$\varepsilon_{\text{el,100}}$ at N_{fat} of 100.000 (µm/m)	19		26		36.8	
	MV	SD	MV	SD	MV	SD
$|E^*|$ (MPa) at 20°C, 10 Hz	6329	1458	7811	752	23.4	−48.4

Table 6.   High-temperature results: path-controlled compaction.

	$H-X-X$		$H-Y-Y$		$H-Z-Z$		$\Delta_{X-X/Y-Y}$ (%)		$\Delta_{Y-Y/Z-Z}$ (%)		$\Delta_{X-X/Z-Z}$ (%)	
	MV	SD	MV	SD	MV	SD	MV	SD	MV	SD	MV	SD
f_{c} (µm/m/n)	−0.373	0.024	−0.285	0.004	−0.277	0.075	−23.6	−83.3	−2.8	1775	−25.7	212.5

Table 7.   High-temperature results: force-controlled compaction.

	$H-X-X$		$H-Y-Y$		$H-Z-Z$		$\Delta_{X-X/Y-Y}$ (%)		$\Delta_{Y-Y/Z-Z}$ (%)		$\Delta_{X-X/Z-Z}$ (%)	
	MV	SD	MV	SD	MV	SD	MV	SD	MV	SD	MV	SD
f_{c} (µm/m/n)	−0.414	0.038	−0.270	0.046	−0.208	0.012	−34.8	21.1	−23.0	−73.9	−49.8	−68.4

carried out at a test temperature of 50°C and a frequency of 3 Hz. The axial load ranged from 150 to 750 kPa, and the confining pressure was set to 150 kPa. Thus, the stress deviator ranged from 0 to 600 kPa. For each test procedure, three specimens were tested.

As a result, a relationship between the number of load cycles and the permanent axial strain is derived. A power function is used to describe the loading–strain curve. To compare different mixes, the creep rate (f_c) is obtained indicating the increase in permanent deformation in µm/m per load cycle. The creep rate represents the exponent of the power function. The smaller the absolute value of the creep rate, the better is the high-temperature performance.

For the high-temperature performance, not only different orientations of testing versus compaction were analysed but also different methods of compaction (path- vs. force-controlled compaction).

4.3.1 *Results: path-controlled compaction*

In this test, the $H-Z-Z$ orientation represents the load situation in a pavement structure. The traffic load and the main orientation of reaction (permanent deformation) occur in the direction of the compaction force (Z).

The results for path-controlled compaction are presented in Figure 5. The $H-Y-Y$ and $H-Z-Z$ configurations show similar results with slightly higher resistance to permanent deformation for the $H-Z-Z$ specimens ($+3\%$) and also a far larger scattering in results. The $H-X-X$ orientation produces the highest creep rate and largest permanent deformations. The creep

rate for the $H-Z-Z$ is 26% lower and for the $H-Y-Y$ 24% lower than for the $H-X-X$ (Table 6).

As the TCCT is a test in which the specimen is loaded similarly as during compaction, part of the difference in the performance might be connected to the compaction effort. Thus, Figure 6 compares the bulk density (derived according EN 12697-6, saturated dry surface) and its variation of the path-controlled compacted TCCT speci- mens. Comparing the creep rates (right diagram in Figure 5) with the bulk density, there is no interrelation between the MV of the bulk density and the creep rates. But another interesting trend is described. The larger the variation of the bulk density, the larger is the variation of the creep rates. Thus, the difference in the creep rate between the three test orientations seems to be connected to anisotropy of the material, whereas the scattering of the test results within one test series is linked to variation of the compaction quality itself.

4.3.2 *Results: force-controlled compaction*

Analogue to the results of the path-controlled compaction, the same trend can be derived when testing forced- controlled compaction (Figure 7). $H-X-X$ shows the poorest resistance to permanent deformation, followed by $H-Y-Y$ (35%). $H-Z-Z$ (50%) again produces the smallest creep rate. The variation in the results is similar for the $H-X-X$ (SD: 0.038) and $H-Y-Y$ (SD: 0.046) configuration and significantly lower for the $H-Z-Z$ (SD: 0.012) orientation. This is a difference to path-controlled compaction (Table 7).
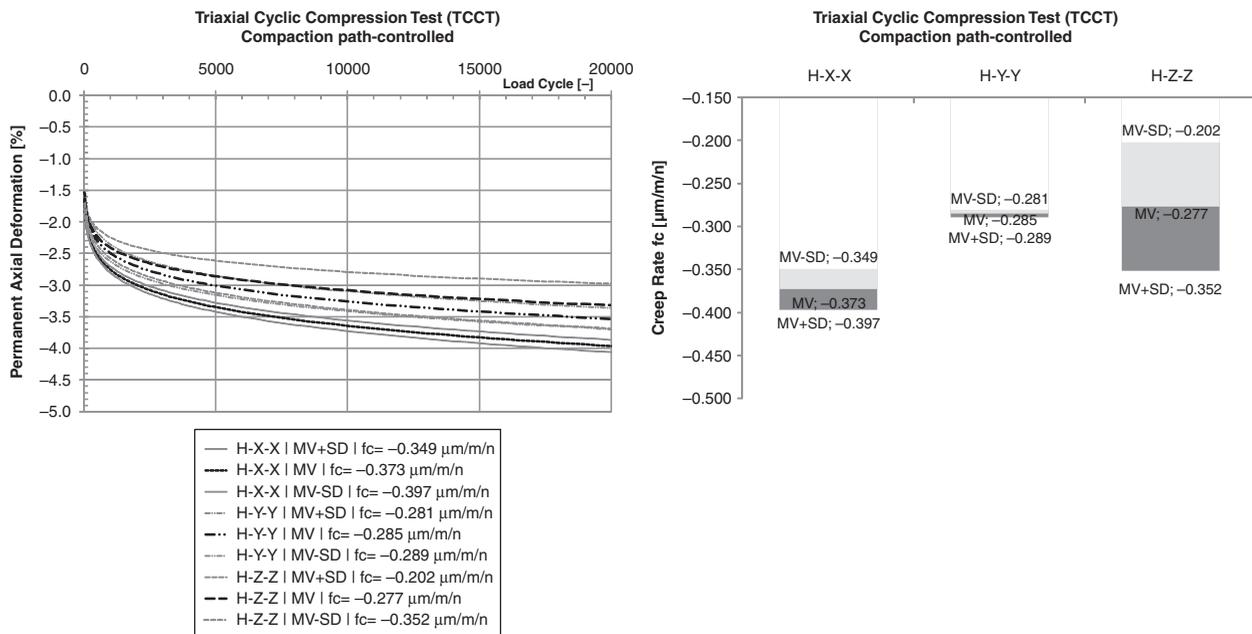
Figure 5.   TCCT results for path-controlled compaction: creep curve (left) and creep rate (right).
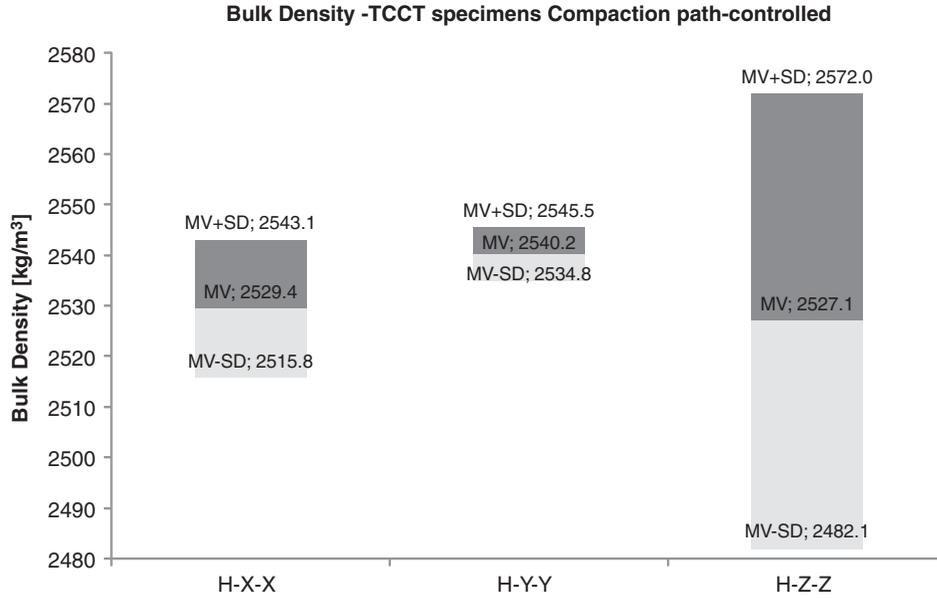
Figure 6.   Bulk density of path-controlled compacted TCCT specimens.

Again the bulk density of the specimens is depicted in Figure 8. Compared with the bulk density of the path-controlled compaction (Figure 6), the variation of specimens from different slabs is quite smaller. This can be explained by the fact that the force-controlled compaction applies the same amount of compaction work into each slab. As the difference in the bulk density of different slabs is not significant, the difference in the calculated creep rate seems to be related to the anisotropy of the material due to compaction.

4.3.3   *Path- versus force-controlled compaction*

Figure 9 compares the results of path- and force-controlled compaction. As the mix design of all produced slabs is the same, the difference between path- and force-controlled slabs should be linked to the compaction work applied to each slab. Thus, the specific compaction work for each slab was calculated. The compactor records the compaction force and path for each cycle. By integrating the compaction force (N) over the compaction path (mm) and dividing it first by the length of the compaction path (mm)
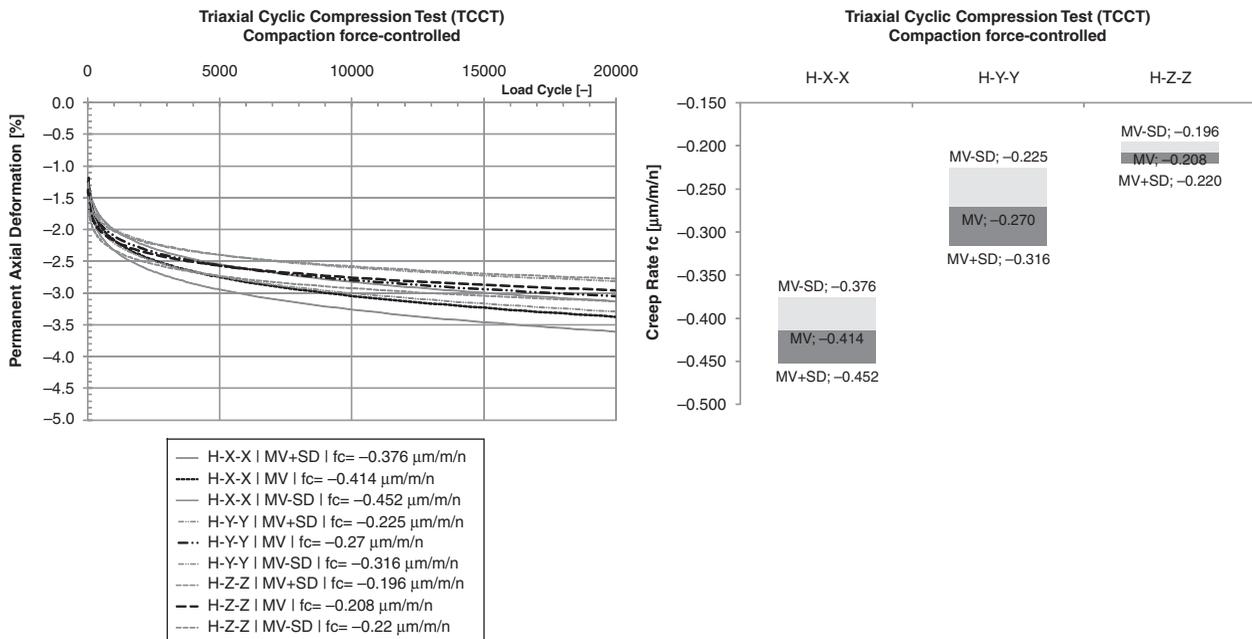
Figure 7.   TCCT results for force-controlled compaction: creep curve (left) and creep rate (right).
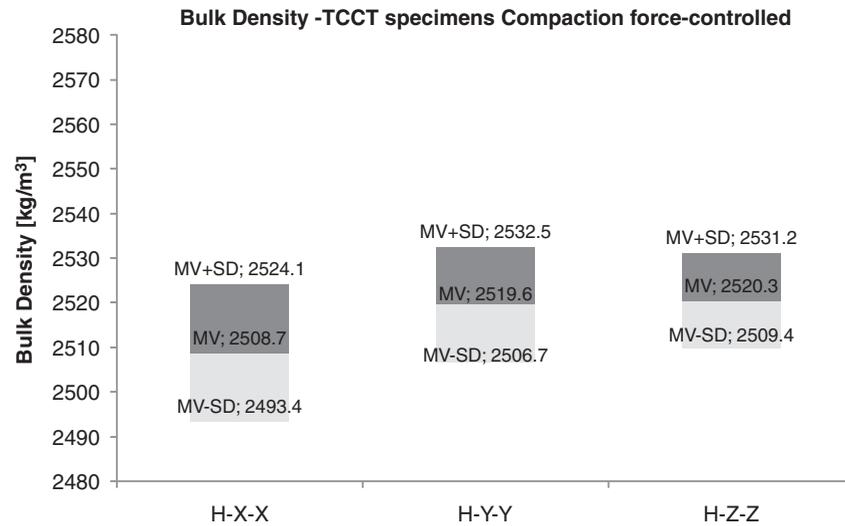
Figure 8. Bulk density of force-controlled compacted TCCT specimens.

and then by the height of the compacted slab (mm), a specific compaction work (N mm/mm^2) can be derived. This parameter is compared in Figure 10.

Starting with $H-Z-Z$, a higher compaction work produces a higher resistance to permanent deformation. The force-controlled compacted slab was produced with a 19% higher compaction work leading to a 25% lower creep rate.

For the $H-X-X$, a higher compaction work leads to a higher creep rate. For the force-controlled compacted slab, a 14% higher input in compaction work is calculated, and yet it shows a poorer resistance to permanent deformation with a 11% higher creep rate. The $H-Y-Y$ configuration shows only a slight sensitivity to the applied compaction work. The path-controlled compacted slab with a 3% higher compaction work leads to a 5% higher creep rate. Specimens tested in the direction of the compaction force (Z) with a higher compaction work result in smaller creep rates. For specimens tested in x- and y-direction, the

situation is vice versa. Taking into account that a higher degree of compaction leads to a situation in which more aggregates are oriented in the $x-y$ plane, it is assumed that when specimens are tested in x- or y-direction, a higher compaction work is counterproductive because more aggregates can slide past each other rather than being resistant to deformation – especially at high temperature when the mastic has lost most of its capacity to transfer load. This thesis is based on limited data and needs to be verified by further testing.

5. Summary and conclusions

This study analyses the impact of the orientation of compaction on the performance parameters of HMA specimens. Test specimens were cut and cored from slabs that were compacted by roller compactor according to EN 12697-33 (2007). To fully describe the performance
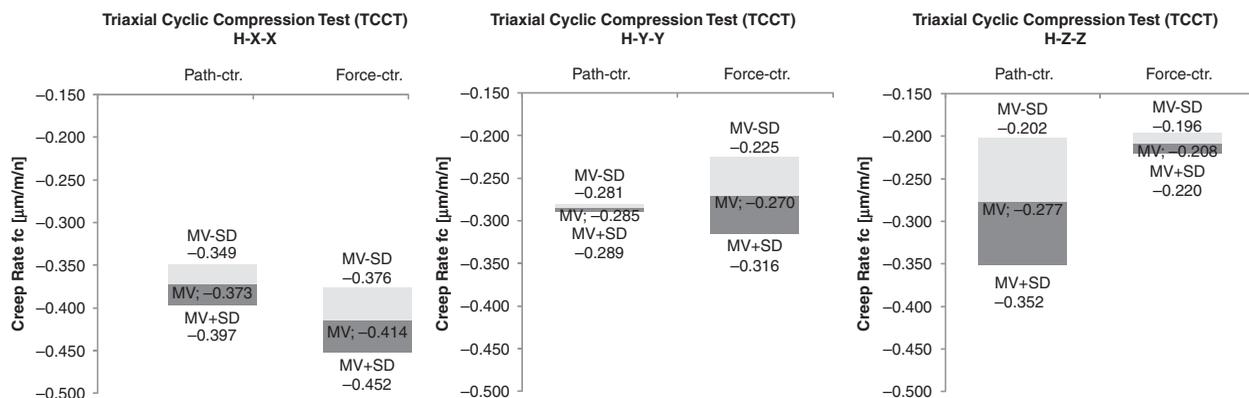
Figure 9. TCCT results – path- versus forced-controlled compaction: creep rates.
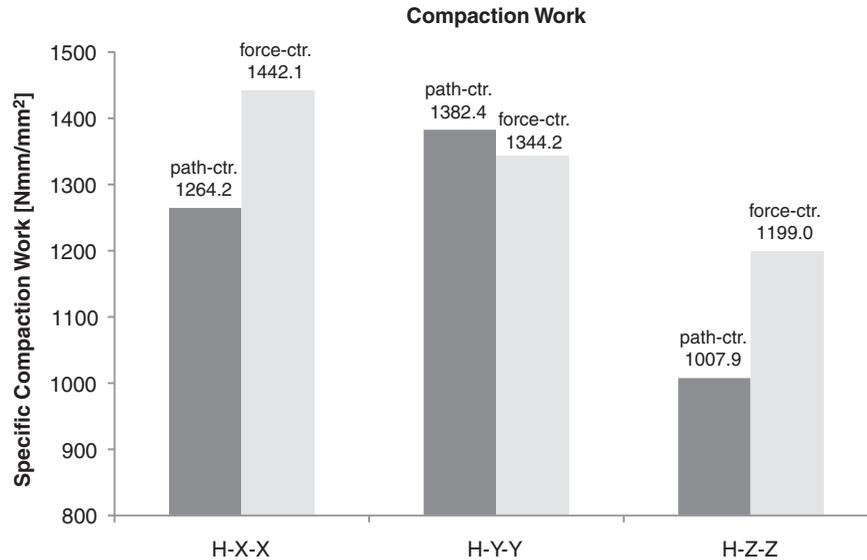
Compaction Work

Figure 10. Compaction work of HMA slabs used for TCCT specimens.

behaviour of the mix, the test programme included the following test methods:

- high-temperature (TCCT according to EN 12697-25),
- stiffness and fatigue (IT-CY according to FGSV AL Sp-Asphalt 09 and EN 12697-24) and
- low-temperature (TSRST and UTST according to prEN 12697-46 (2009)).

Specimens were cut and cored out of the slabs in different patterns (i.e. orientation of specimen testing vs. orientation of compaction). For the high-temperature performance, the compaction method was varied as well to compare path- and force-controlled compaction. Low-temperature and fatigue and stiffness tests were carried out only on path-controlled compacted specimens. Summing up the results, the following findings can be given:

- The low-temperature performance is moderately sensitive to the material anisotropy. Specimens tested in the *x*-direction (orthogonal to compactor path and compaction force) perform better than specimens tested in the *y*-direction (in direction of compactor path orthogonal to compaction force) with lower cracking temperatures in the TSRST and a higher tensile strength reserve.
- The stiffness and fatigue performance is highly sensitive to the material anisotropy. The tested $F-Z-Y$ orientation reflecting the loading situation on the road was about 23% stiffer than the $F-X-Y$ direction (at 20°C and 10 Hz) and resulted in a better fatigue performance (+36%).
- The high-temperature performance was assessed for all three orientations and for path- and force-controlled compaction. For both compaction

methods, an anisotropic performance was found. In this test, part of the difference in performance might be connected to the compaction effort itself. Therefore, the bulk density of the tested specimens was compared with the calculated creep rates. Interestingly, the larger the variation of the bulk density, the larger the scattering in the creep rates is. The different creep rates in the three test directions seem to be connected to anisotropy of the material, whereas the variation of the results is linked to the variation of the compaction quality itself. Best performance was found for specimens tested in the direction of the compaction force (*Z*), which reflects the loading situation on the road followed by *y*- and *x*-orientation.

- Comparing the results of path- and force-controlled compaction in terms of the high-temperature performance, it seems that the applied compaction work rather than the compaction method is linked to the difference in path- and force-controlled compaction. For the *z*-direction, a higher compaction work results in smaller creep rates. For the *x*- and *y*-direction, a lower compaction work produces smaller creep rates. It is assumed that a higher degree of compaction leads to a situation where more aggregates are oriented in the *x*–*y* plane. Thus, when specimens are tested in *x*- and *y*-direction, a higher compaction work does not lead to a decrease in the resulting creep rate because aggregates would slide past each other rather than being resistant to deformation. This is especially true at high temperatures when the mastic has lost most of its capacity to bear loads. This thesis is based on very limited data and needs to be verified by further testing.

From the results, the following conclusions can be drawn:

- When specifying performance indicators of HMA by laboratory testing, the specimen preparation and orientation of testing have a crucial influence on the results for the entire temperature range as the performance is sensitive to the material anisotropy due to compaction.
- Specimens in the laboratory are often cut and cored out of slabs in a way that is most economic and efficient in terms of material use and easy to handle specimen preparation. More care needs to be put on the fact that specimens should be tested in the same orientation as the pavement structure is stressed under traffic and climate loading if the performance indicators produced by sophisticated test procedures should reflect reality in the most reliable way. This is especially true for high-temperature and fatigue and stiffness testing.
- This fact is even more important when the material parameters determined by laboratory testing should be implemented into modelling and simulation (Hofko and Blab 2009). The anisotropic performance must be taken into account to obtain realistic simulation results.
- An influence of the compaction method (path- vs. force-controlled compaction) on the performance indicators at least in the high-temperature range was not found in this study. Differences in results are rather linked to the compaction work applied during compaction of the slabs. A higher compaction work leads to better deformation resistance in the *z*-direction and a lower resistance in the *x*- and *y*-direction. The uniformity of the compaction in terms of variation of bulk density of the specimens reflects on the scattering of test results.

Notes

1. Email: ronald.blab@tuwien.ac.at
2. Email: a.alisov@tu-bs.de

References

Airey, G.D., Collop, A.C., and Zoorob, S., 2005. *The influence of laboratory compaction methods on the performance of asphalt mixtures*. Final Report. Engineering and Physical Science Research Council.

Brown, S.F. and Gibb, J.M., 1999. *Effects of compaction on mechanical properties of asphalt mixtures*. Proceedings of the 7th conference on asphalt pavement for Southern Africa, Victoria Falls, Zimbabwe.

EN 12697-24, 2007. Bituminous mixtures – Test methods for hot mix asphalt – Part 24: Resistance to fatigue.

EN 12697-25, 2006. Bituminous mixtures – Test methods for hot mix asphalt – Part 25: Cyclic compression test.

EN 12697-33, 2007. Bituminous mixtures – Test methods for hot mix asphalt – Part 33: Specimen prepared by roller compactor.

EN 12697-35, 2007. Bituminous mixtures – Test methods for hot mix asphalt – Part 35: Laboratory mixing.

EN 13108-1, 2006. Bituminous mixtures – Material specifications – Part 1: Asphalt concrete.

FGSV AL Sp-Asphalt 09, 2009. Arbeitsanleitung zur Bestimmung des Steifigkeits – und Ermüdungsverhaltens von Asphalten mit dem Spaltzug-Schwellversuch als Eingangsgröße in die Dimensionierung [Determination of stiffness and fatigue behavior of asphalt mixes by indirect cyclic tension testing] (in German).

Hofko, B. and Blab, R., 2009. *Performance based lab tests to predict pavement fatigue*, Proceedings of the fifth international conference on construction in the 21st century, Paper-Nr. 171, Istanbul, Turkey.

Hunter, E.A., Airey, G.D., and Collop, A.C., 2004. Aggregate orientation and segregation in laboratory-compacted asphalt samples. *Journal of the Transportation Research Board*, 1891, 8–15.

Iwama, M., Airey, G.D., and Hunter, A.E., 2007. Influence of asphalt mixture compaction method and specimen size on internal structure and mechanical properties. *In*: *Proceedings of the international conference on advanced characterisation of pavement and soil engineering materials*. Athens: CRC Press, 1063–1073.

Masad, E., *et al.*, 1999. Quantifying laboratory compaction effects on the internal structure of asphalt concrete. *Journal of the Transportation Research Board*, 1681, 179–185.

Masad, E., *et al.*, 2002. Micromechanics-based analysis of stiffness anisotropy in asphalt mixtures. *Journal of Materials in Civil Engineering*, 14 (5), 374–383.

prEN 12697-46, 2009. Bituminous mixtures – Test methods for hot mix asphalt – Part 46: Low Temperature Cracking and Properties by Uniaxial Tension Tests.

Renken, P., 2000. Influence of specimen preparation onto the mechanical behaviour of asphalt mixtures. *In*: *Proceedings of the 2nd Eurasphalt & Eurobitume congress, Session 1: Performance testing and specifications for binders and mixtures.* Barcelona, Spain: European Asphalt Pavement Association, 729–735.